

Open Access Article



<https://doi.org/10.55463/issn.1674-2974.50.2.7>

## A Hybrid GWO-MPO-Based Maximum Power Point Tracking for Photovoltaic System for a New MLI with Minimum Number of Switches

Hussein S. Abdulazeez\*, Rabee' H. Thejel, Diyah K. Shary

Department of Electrical Power Techniques Engineering, Southern Technical University, Iraq

\* Corresponding author: [h.s.abdulazziz@stu.edu.iq](mailto:h.s.abdulazziz@stu.edu.iq)

Received: December 18, 2022 ▪ Review: January 4, 2023 ▪ Accepted: February 10, 2023 ▪ Published: February 27, 2023

**Abstract:** Photovoltaic (PV) systems provide a number of challenges, one of the most critical of which is determining how to extract the maximum amount of usable power from the PV system even when the system is running in conditions of fast change in irradiance. This study aims to demonstrate a novel hybrid approach to maximum power point tracking (MPPT), which is built on the grey wolf optimization algorithm (GWO) and modified perturb and observe (MP&O) techniques. The second goal of this method is to provide a robust MPPT method with minimum losses in the MPP point of the PV module. This technique is based on the connection of a single KC200GT PV module. The KC200GT PV module is connected to the DC bus via DC/DC boost converter to raise the voltage and implement the MPPT algorithm. After that, the PV system was integrated to supply a new multilevel inverter (MLI) with a reduced number of switches. Additionally, the MATLAB/Simulink environment was used to demonstrate and evaluate the efficacy of the proposed MPPT approach. Complex fast changes in solar irradiation are applied to the module to verify the feasibility and efficacy of the hybrid method by comparing its performance to that of the P&O, and MP&O algorithms. The obtained results demonstrated that the hybrid GWO-MP&O MPPT method achieved an excellent level of efficacy in terms of MPP accuracy, convergence speed (0.05 sec), and overall tracking efficiency (99.7%) compared to other approaches.

**Keywords:** Grey Wolf Optimizer, maximum power point, boost converter, photovoltaic system, multilevel inverter, perturb and observe.

### 基于混合GWO-MPO的光伏系统最大功率点跟踪，适用于具有最少开关数量的新型多边语言

**摘要：**光伏系统面临许多挑战，其中最关键的挑战之一是确定如何从光伏系统中提取大量的可用功率，即使系统在辐照度快速变化的条件下运行也是如此。本研究旨在展示一种新的最大功率点跟踪混合方法，该方法建立在灰狼优化算法和改进的扰动观察技术之上。该方法的第二个目标是提供一种稳健的最大功率点跟踪方法，使光伏模块的最大功率点损失最小。该技术基于单个KC200GT光伏模块的连接。KC200GT光伏模块通过直流/直流升压变换器连接到直流母线，提升电压，实现最大功率点跟踪算法。之后，集成了光伏系统以提供开关数量减少的新型多级逆变器。此外，还使用软件/仿真链接环境来演示和评估所提出的最大



功率点跟踪方法的功效。将太阳辐射的复杂快速变化应用于模块，通过将其性能与常规扰动观察和改进的扰动观察算法进行比较，验证混合方法的可行性和有效性。获得的结果表明，混合灰狼优化-

修正扰动和观察最大功率点跟踪方法在最大功率点精度、收敛速度（0.05秒）和整体跟踪效率（99.7%）方面取得了优异的效果。其他方法。

**关键词：**灰狼优化器、最大功率点、升压转换器、光伏系统、多电平逆变器、扰动观察。

## 1. Introduction

In recent few years, renewable energy, and solar energy in particular, is a significant and potential alternative power source for electric power production. Solar power is a great option since it may provide unlimited, clean energy with no environmental impact. Compared to other types of energy, it is the most readily available [1, 2]. Solar-to-electricity conversion has various potential uses, including transportation, marine, residential, aviation, and spacecraft [3]. This is why many people believe that solar energy will play a significant role in the global electricity production in the next decades. The usage of a photovoltaic (PV) system is one way to collect this energy [4, 5]. PV systems may be used independently or tied into the main power supply. It is certain that the penetration of PV systems on the utility grid or standalone operation will expand further, particularly on low and medium-voltage grids [6].

Moreover, the rapidly decreasing cost of PV modules, improvements in power electronics, and government incentives toward PV systems. Researchers are looking into more advanced PV systems to find ways to make and use PV systems that work better [7, 8]. Maximum power point tracking (MPPT) control is one of the developed methods for increasing the efficiency of PV systems. The MPPT is a device consisting of DC/DC converter and a suitable MPPT algorithm embedded in a microcontroller. Many factors, including cost, reaction time, complexity, oscillation around the MPP, and sensors, must be considered when deciding on an MPPT method. Such methods include perturb and observe (P&O) [9, 10], Incremental Conductance (INC) [11, 12], and Hill Climbing (HC) [13]. Unfortunately, these methods fell short when trying to precisely monitor the global maximum power point (GMPP) under varying levels of irradiance. Additionally, these methods, do not discriminate between the GMPP and a local MPP (LMPP) when the partial shading conditions (PSCs) occur. As a result, various MPPT-based optimization techniques have recently been published to predict the GMPP and improve the PV array's efficiency under PSCs. Such algorithms include: Genetic Algorithm

(GA) [14], Cuckoo Search (CS) [15, 16], Particle Swarm Optimization (PSO) [17, 18], Ant Colony Optimization (ACO) [19], and Mine Blast Optimization (MBO) [20]. Besides, it has been observed from previous studies that most researchers have considered just a single optimization algorithm to detect the GMPP under PSCs. Nonetheless, optimization strategies grounded on swarm intelligence (SI) such as ant bee colony (ABC) [21], ACO, and PSO have been used in the creation of MPPT controllers as well. They have substantial advantages, such as less computational effort and independence from intrinsic system factors, but they lack flexibility due to this necessity. However, earlier studies propose hybrid methods that boost the efficiency of the PSO-based MPPT algorithm when dealing with PSCs in PV plants, such as the ABC with PO (ABC-PO) [22] and the PSO with P&O (PSO-PO) [23].

Grey wolf optimization algorithm (GWO) is one of the SI family that emulates the hierarchy leadership and hunting technicality of grey wolves as proposed by Mirjalili et al [24]. The GWO-based MPPT is used in different studies to track the MPP and then increase the performance of the solar systems under uniform and non-uniform irradiation conditions. The authors in [25] proposed a hybrid GWO-PO-based MPP to enhance the performance of the PV modules under PSCs. This hybridization-based P&O algorithm, which has several issues such as low response, and failure under a fast change in irradiation. For this reason, the GWO algorithm is integrated with a modified PO (MPO) method to increase the PV system's efficiency under normal and PSC conditions. Moreover, to the author's knowledge, there is no previous work in the literature that deals with the hybrid GWO-MPO for MPPT in PV systems. In addition, the proposed technique directly modifies the duty cycle without the need to use a linear compensator in this work's MPPT controller, which simplifies the process and removes any computing overhead with adjusting the compensator gains. With these advantages, the suggested GWO-MPO-based MPPT technique can be seen as a promising prospect for PV systems working in both uniform and non-uniform irradiance circumstances.

The novelty of this paper is seeking to contribute to the new hybrid MPPT method and the following finding clearly this novelty:

1. Propose a new MPPT-based GWO and MP&O methods.
2. Increase the efficiency of the PV module under different weather conditions.
3. Minimize the power fluctuation under fast changes in irradiance.
4. Present a new MLI with a minimum number of switches.

## 2. Proposed System Description

### 2.1. System Structure

Fig. 1 displays the proposed PV system structure along with DC/DC power converter (boost converter), the PV panel type KC200GT (200 W), the proposed hybrid GWO-MP&O based MPPT, MLI with a minimum number of switches, the inverter's control scheme, and output load. The PV module is managed and interfaced with the boost converter circuit to apply the MPPT algorithm that is based on the suggested GWO-MP&O MPPT controller.

By using the DC/DC boost converter in this situation, the aim is to enhance and increase the output voltage of the PV system from 26.3 V to 100 V on the DC bus side. In addition, the goal of the PWM control is to provide a suitable sinusoidal PWM pulse for the proposed MLI inverter. The resistive load is connected with the inverter using seven levels of the output voltage.

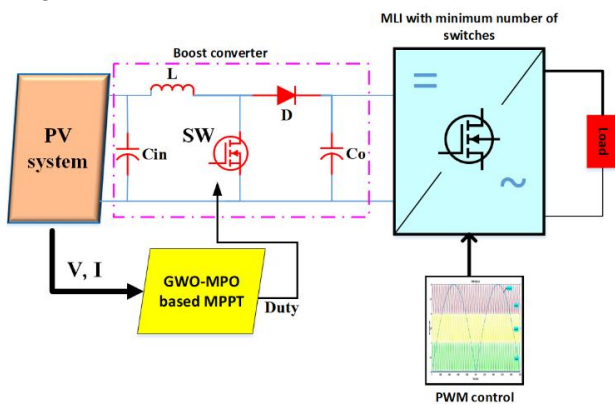


Fig. 1 The proposed system structure

### 2.2. Photovoltaic Module Model

By virtue of the photovoltaic effect, the PV cell accomplishes the direct transformation of solar energy into electrical energy. Since a typical PV cell generates between 1 and 2 watts of electricity [26], the output power of PV cells may be increased by configuring the cells into modules. As a result, the model of a single diode, which can be shown in Fig. 2, is used in this study, which considers the most equivalent circuit for the PV cell or module [27]. This model represented by the photocurrent, diode, parallel resistor, and series

resistor. The output current of the module can be given as in Equation 1.

$$I_{PV} = N_P I_{ph} - N_P I_0 \left[ \exp \left[ \frac{q}{VKT} \left( \frac{V_{PV}}{N_S} + \frac{I_{PV} R_{sm}}{N_P} \right) \right] - 1 \right] - \frac{N_P}{R_{pm}} \left( \frac{V_{PV}}{N_S} + \frac{I_{PV} R_{sm}}{N_P} \right) \quad (1)$$

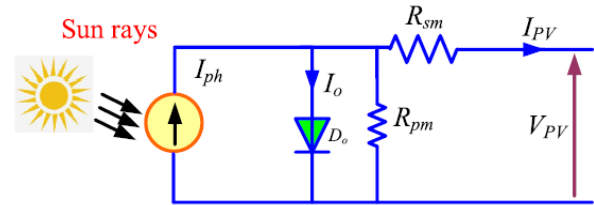


Fig. 2 Single-diode model of the PV module [27]

The above items can be represented by the following description:

- $I_{PV}$  - the array's current.
- $V_{PV}$  - the array's voltage.
- $I_{ph}$  - the photo current of the array.
- $I_o$  - the diode current in the case of saturation.
- $R_{sm}$  - the series resistor.
- $R_{pm}$  - the parallel-resistor
- $T$  - the ambient temperature.
- $N_P$  - the number of parallel strings.
- $N_S$  - the number of module strings.
- $V$  - the thermal voltage.
- $K$  - the Boltzmann constant ( $1.380653 \times 10^{-23} J/K$ ).
- $q$  - the electron's charge ( $1.60217646 \times 10^{-19} C$ )

As discussed before, in this work, one PV module of KC200GT with 200 W was used to test and verify the proposed hybrid MPPT. The specification of this module under standard test conditions (STC) can be seen in Table 1.

Table 1 Technical electrical datasheet specification of the KC200GT Panel

Parameter	Description
$P_{max}$	200 W
$V_{max}$	26.3
$I_{max}$	7.6 A
$V_{oc}$	32.9 V
$I_{sc}$	8.21 A
$k_v$	-80 mA/C
$k_i$	2 mV/C
$N_{ser}$	54

Fig. 3 shows the I-V and P-V characteristics of the KC200GT under different values of irradiance. Also, the I-V and P-V curves of this module under different temperatures can be shown in Fig. 4. As seen in these figures, the solar current is very sensitive to solar

irradiation and this current is decreased by a reduction in the irradiance. The maximum power of 200 W is achieved under  $G = 1 \text{ kW/m}^2$ , and  $T = 25 \text{ }^\circ\text{C}$ , where  $T$  is the temperature and  $G$  is the solar irradiance.

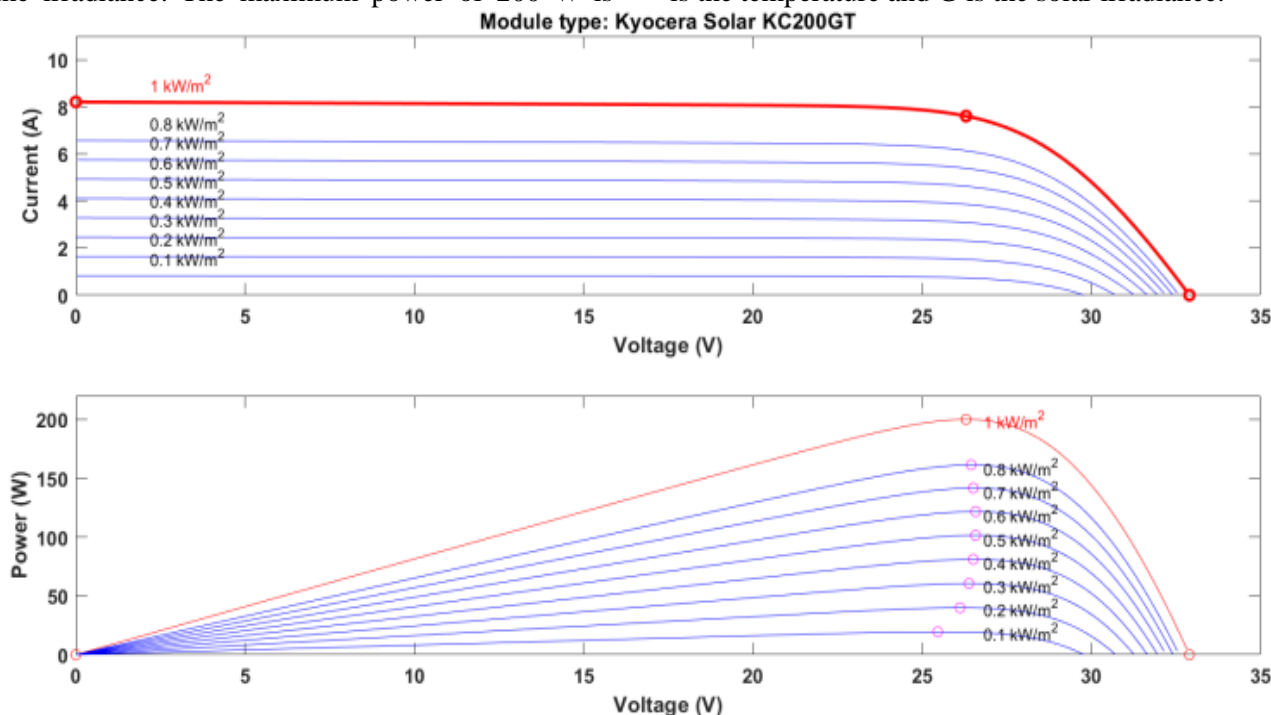


Fig. 3 The I-V and P-V characteristics of the KC200GT under different values of irradiance

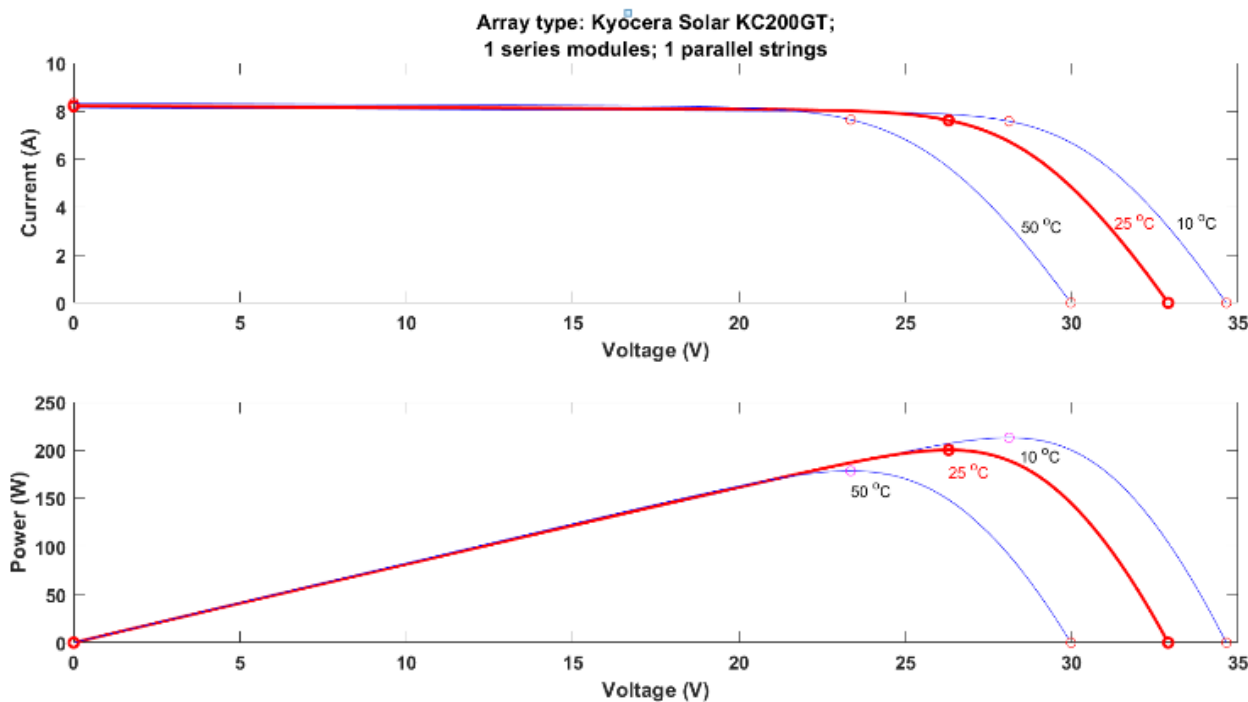


Fig. 4 The I-V and P-V characteristics of the KC200GT under different values of temperature

### 2.3. DC/DC Boost Converter Design

The DC/DC boost converter is installed in the space between the panel and the multilevel inverter to the load, and it is controlled by the MPPT controller with the use of a duty cycle [28, 29]. This invention intends to rectify the imbalance that currently exists between the PV panel and the load so that the PV panel may perform at its maximum possible efficiency. The electrical circuit of the boost converter is simple and easy to modeling. The simplicity and the low cost may

be established are perhaps the most significant benefit of using a boost converter. As seen in Fig. 1, the boost converter circuit consists of a switch such as MOSFET or IGBT, diode, inductor, input capacitor, and output capacitor. The modeling of this converter is performed based on the following equations [29]:

$$L_b = \frac{V_{PV} D}{f_s \Delta I_{PV}} \quad (2)$$

$$C_{in} \geq \frac{D}{8 \times f_s^2 \times L_b \times 0.01} \quad (3)$$

$$C_{out} = \frac{I_o D}{f_s \Delta V_o} \quad (4)$$

where  $L_b$  is the inductance,  $C_{in}$  is the input capacitor which is used to filter the voltage of the PV voltage,  $C_{out}$  is the output capacitor,  $D$  is the duty ratio,  $I_o$  is the output current of the boost converter,  $\Delta V_o$  is the ripple in the output voltage,  $f_s$  is the switching frequency, which is 5000Hz. The parameters of this design are:

$$L_b = 0.1 \text{ mH}, C_{in} = 1000 \text{ uF}, \quad \text{and } C_o = 1000 \text{ uF}.$$

#### 2.4. Design of the Modified P&O Method

In the research done, many MPPT algorithms have been used to extract the greatest amount of power that can be obtained from the PV panel in response to varying amounts of solar irradiation. The P&O algorithm is the ones that are used the most often. This algorithm is designed to change the duty cycle of a boost converter in such a manner that boosted DC voltage may be achieved [30]. This is accomplished by maximizing the efficiency of the boost converter. The perturbation ( $\Delta D$ ) that is introduced by P&O must either have variable step sizes or fixed step sizes to attain the maximum power point. Alterations in the intensity of the radiation might cause problems. The oscillation gives the impression of being in a stable state when the step size ( $\Delta D$ ) is kept constant as seen in the conventional flowchart of Fig. 5. On the other hand, a variable step size will determine the step sizes for automatically, which will lead to less oscillations and faster tracking [30]. In this particular piece of research, made the advantage of a variable step size while working with P&O.

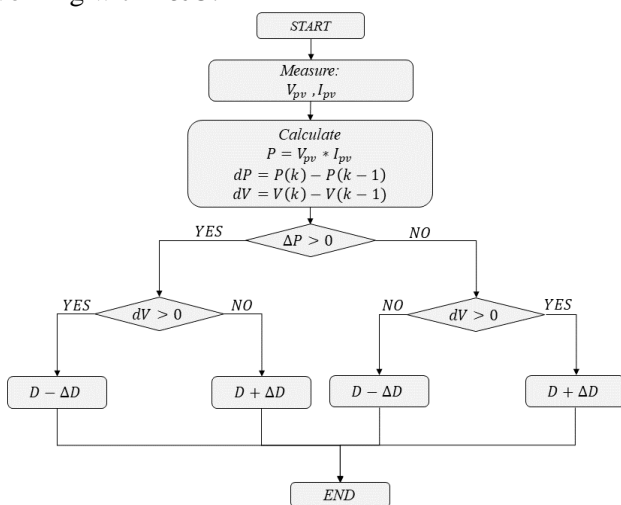


Fig. 5 Flowchart of the conventional P&O MPPT [30]

The MP&O is modified by sensing the change in the output power of the PV module and updating the perturbation based on the following equation:

$$\Delta D = \Delta D(0) \cdot |dP| \quad (5)$$

where  $\Delta D(0)$  is the initial perturbation of the duty

cycle, and  $dP$  is the change in the PV power at any irradiance.

To design the MP&O method, the current and voltage of the PV must first be measured. Next, the power is computed and compared to the power that is previously measured. The algorithm produces a perturbation ( $\Delta D$ ) in the duty cycle in response to a change in the PV power. Also, another modification is done in this work, which is modified-loop to avoid the fast ripple in the power due to the quick varying in the irradiance. This can be seen in the flowchart below. As shown, the left side of the MP&O flowchart is added here to make the technique faster than the conventional P&O. The MP&O algorithm's flowchart is shown in Fig. 6.

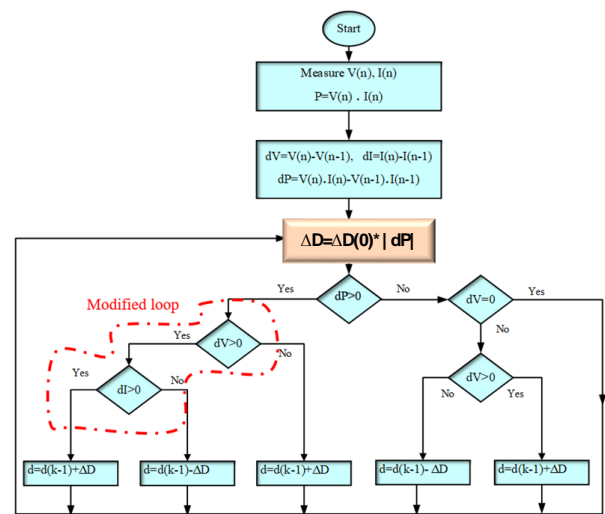


Fig. 6 Flowchart of the MP&O MPPT

#### 2.5. Proposed Hybrid MPPT Method

As described by Mirjalili et al. [24], GWO is a metaheuristic algorithm that simulates the hierarchy, leadership, and hunting technique of gray wolves. The proposed MPPT is designed, as seen in Fig. 7. This work aims to integrate both GWO optimization with modified P&O-based MPPT techniques. The advantage of the GWO is to detect the global MPPT during the partial shading conditions (PSCs), while the MP&O is used to detect the MPP of the module under uniform conditions. The MP&O MPPT approach, however, does not discriminate between a global MPP (GMPP) and a local MPP (LMPP) when applied to the PSCs. This occurs because it concentrates on the MPP, which is almost always a local MPP. Because of this, there is a significant loss of energy, which may reach up to 70%, which is a significant departure from the targeted ideal energy harvesting. As a result, this combination results in a good response with smooth power oscillation. The duty cycle of the proposed hybrid MPPT is achieved by taking the average duty ratio of these techniques after that detecting the output power of the PV module. Accordingly, the change in the power with a threshold value  $P_{(thr)}$  is used to control the duty ratio and minimize the fast change in the duty

cycle that causes more oscillation and slow response. The duty of the hybrid MPPT,  $D_{(H)}$  is written as follows:

$$D_{(H)} = \frac{(D_{(GWO)} + D_{(MP\&O)})}{2} * P_{(thr)} \quad (6)$$

where  $D_{(GWO)}$ ,  $D_{(MP\&O)}$  are the duty cycles of the GWO and MP&O methods, respectively. The  $P_{(thr)}$  is taken in this work less than 4 W. As a result, this condition makes the proposed MPPT more accurate and robust than the conventional techniques.

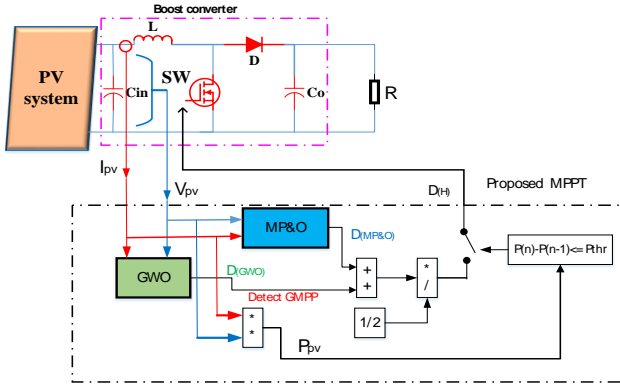


Fig. 7 Hybrid GWO-MP&O-based MPPT method

Furthermore, the design of the proposed MPPT, first the algorithm of the GWO method is analyzed based on the following equations (7-13) [24]. To establish the hierarchy leadership of the grey wolves, this algorithm uses all four levels of leadership available to them. These levels are denoted by their corresponding symbols: omega ( $\omega$ ), beta ( $\beta$ ), delta ( $\delta$ ), and alphas ( $\alpha$ ) [24].

$$\vec{D}_\alpha = |\vec{C}_1 \cdot \vec{X}_\alpha - \vec{X}| \quad (7)$$

$$\vec{D}_\beta = |\vec{C}_2 \cdot \vec{X}_\beta - \vec{X}| \quad (8)$$

$$\vec{D}_\delta = |\vec{C}_3 \cdot \vec{X}_\delta - \vec{X}| \quad (9)$$

$$\vec{X}_1 = \vec{X}_\alpha - \vec{A}_1 \cdot (\vec{D}_\alpha) \quad (10)$$

$$\vec{X}_2 = \vec{X}_\beta - \vec{A}_2 \cdot (\vec{D}_\beta) \quad (11)$$

$$\vec{X}_3 = \vec{X}_\delta - \vec{A}_3 \cdot (\vec{D}_\delta) \quad (12)$$

$$\vec{X}(t+1) = \frac{\vec{X}_1 + \vec{X}_2 + \vec{X}_3}{3} \quad (13)$$

where  $\vec{D}$ ,  $\vec{C}$ , and  $\vec{A}$  represent the vectors of coefficients,  $\vec{X}$  represents the position vector of the grey wolf,  $\vec{X}_\alpha$ ,  $\vec{X}_\beta$ , and  $\vec{X}_\delta$  are the positions of  $\alpha$ ,  $\beta$ , and  $\delta$ , respectively,  $t$  is the current iteration,  $\vec{A}_1$ ,  $\vec{A}_2$ ,  $\vec{A}_3$ ,  $\vec{C}_1$ ,  $\vec{C}_2$  and  $\vec{C}_3$  are random vectors. The general equations for  $\vec{A}$  and  $\vec{C}$  are given in Equations 14 and 15.

$$\vec{A} = 2 \vec{a} \cdot \vec{r}_1 - \vec{a} \quad (14)$$

$$\vec{C} = 2 \vec{r}_2 \quad (15)$$

where  $\vec{a}$  is the ingredient vector that reduces linearly during the iteration process from 2 to 0,  $\vec{r}_1$  and  $\vec{r}_2$  represented by random vectors [0,1]. The update process for the GWO optimizer of search positions in the search space can be seen in Fig. 8. Furthermore, the latest locations are in an arbitrary place in the search space internal a circle, which is performed by the locations of  $\alpha$ ,  $\beta$ , and  $\delta$ . As a result, these factors assess prey positions, while other wolves modernize their locations randomly adjacent to the prey.

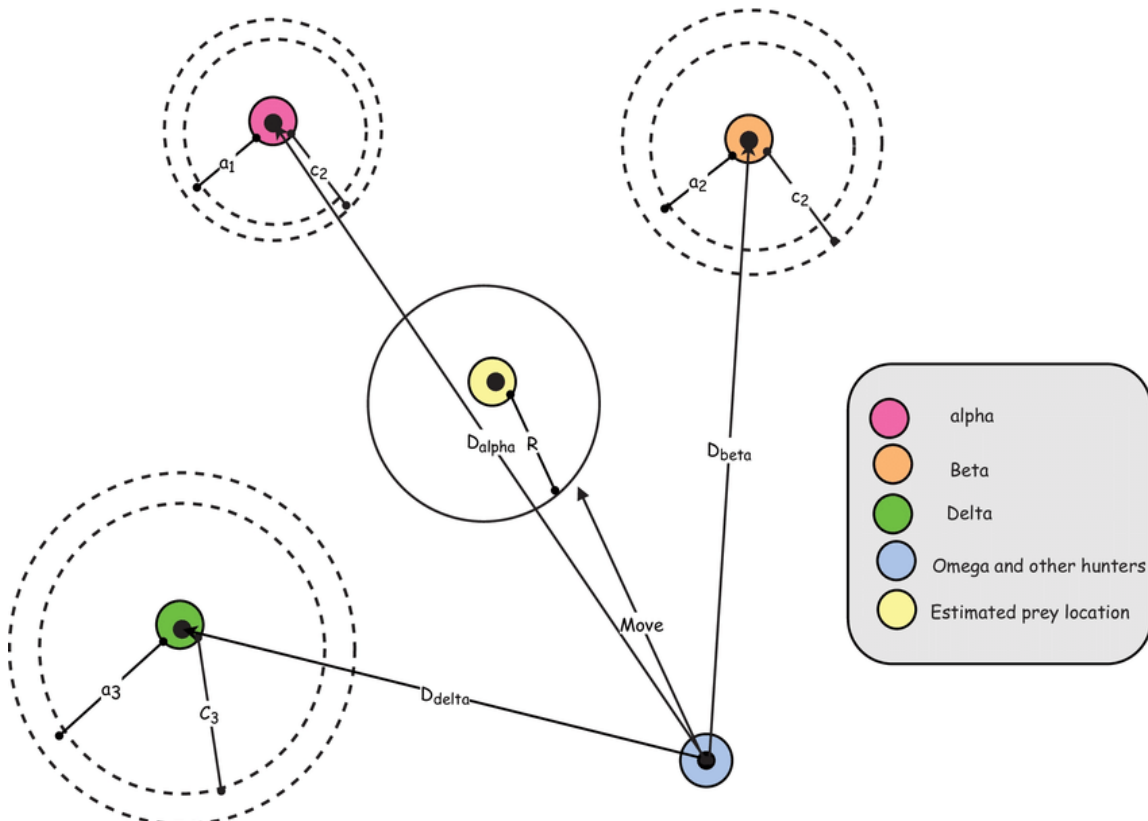


Fig. 8 The update process for the GWO optimizer [24]

The algorithm procedure for the GWO optimization with MP&O can be defined as follows:

- 1) Initial populations in the search space randomly.
- 2)  $\alpha$ ,  $\beta$ , and  $\delta$  wolves appraise the plausible position of the prey via iterations.
- 3) " $a$ " is reduced linearly from 2 to 0 to search for prey and abuse prey, individually.
- 4) Applicant positions tend to move far from the

prey while  $|\vec{A}| > 1$  and join to the prey while  $|\vec{A}| < 1$ , as a result, this keeps away from stagnation in the local solutions.

- 5) The GWO algorithm stops the searching process and sends the best solution to the MPO algorithm when the end paradigm is met.

Fig. 9 displays the flowchart of the proposed GWO-MPO method.

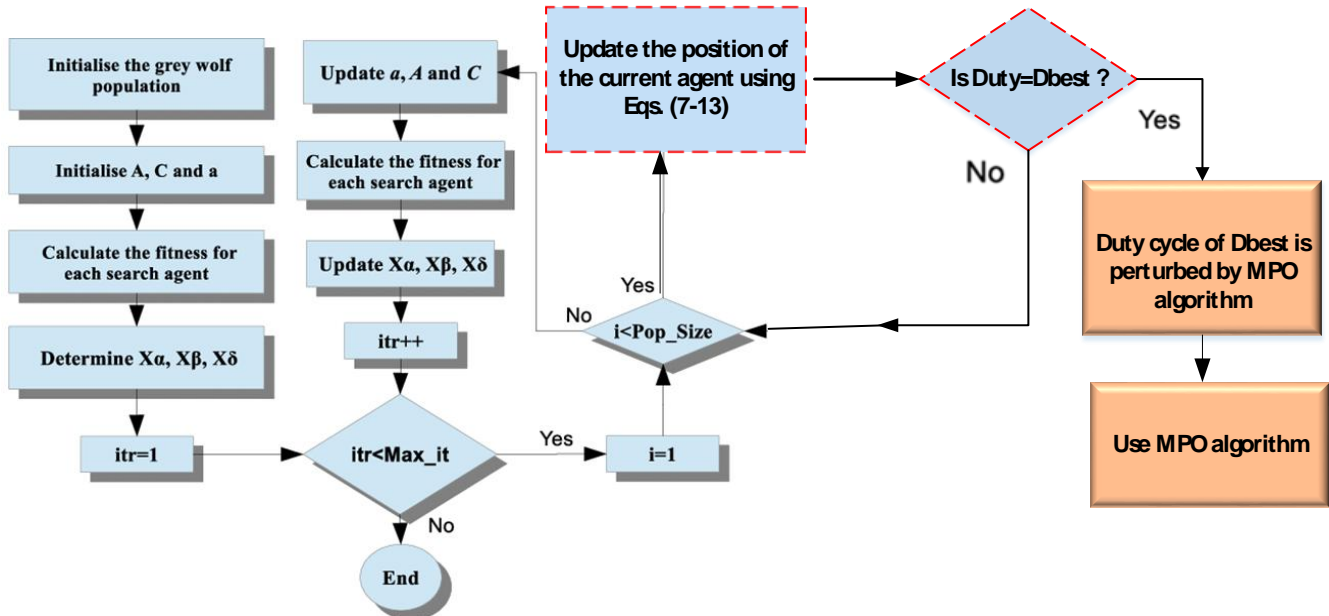


Fig. 9 The hybrid GWO-MP&O MPPT technique

### 3. Proposed MLI with Reduce Number of Switches

Fig. 10 depicts the multilevel construction with a reduced number of switches that has 7 levels and includes a switched capacitor. A single DC supply, eight switches, two diodes, and two capacitors are parts of the suggested inverter. There are four switches complimentary to one another ( $S1$ ,  $S2$ ,  $S3$ , and  $S4$ ). The output of the inverter, denoted by the symbol  $V_{an}$ , is proportional to the source voltage ( $V_d$ ,  $C$ ). The input voltage (DC voltage) is generated from a PV system of three panels in series to study the PSCs and it is the effect on the performance of the proposed MLI.

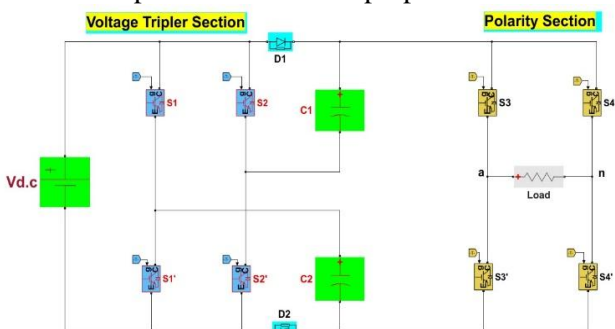


Fig. 10 Proposed 7-level MLI circuit

The proposed MLI is divided into two sections, as shown on the left side of Fig.10; the first component

consists of ( $S1$ ,  $S2$ ,  $S1'$ ,  $S2'$ ,  $C1$ ,  $C2$ ,  $D1$ ,  $D2$ , and source voltage ( $V_d$ ,  $C$ ). This section is responsible for generating the required levels of the output voltage. The second part of the suggested circuit is a polarity part and is used to generate the required single-phase voltage based on the four switches ( $S3$ ,  $S3'$ ,  $S4$ , and  $S4'$ ) that are used to invert the polarity of the component (H-bridge). The modes of operation of switches can be summarized in Table 2.

Table 2 Switching states of a proposed 7-level inverter

States	Tripler circuit	Polarity circuit	Capacitors	$V_{an}$
1	1 0	1 0	Charge Charge	$+V_{dc}$
2	1 1	1 0	Discharge Charge	$+2V_{dc}$
3	0 0	1 0	Charge Discharge	$+2V_{dc}$
4	0 1	1 0	Discharge Discharge	$+3V_{dc}$
5	0 1	0 0	Idle Idle	$0V$
6	1 0	0 1	Charge Charge	$-V_{dc}$
7	0 0	0 1	Discharge Charge	$-2V_{dc}$
8	1 1	0 1	Charge Discharge	$-2V_{dc}$
9	0 1	0 1	Discharge Discharge	$-3V_{dc}$

The circuit control method based on the PWM-type phase dispositions technique is used in this paper, as seen in Fig. 11. The proposed control method is based on some logic gates and comparators. The sinusoidal waveform is used to extract the rectified wave, and then this signal is compared with the waveforms based on triangles with the same frequency and phase as seen

in Fig. 12.

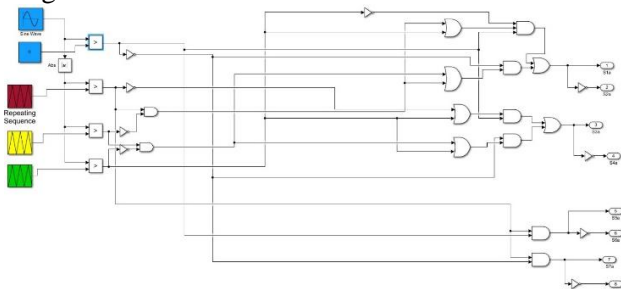


Fig. 11 The circuit control method based on PWM

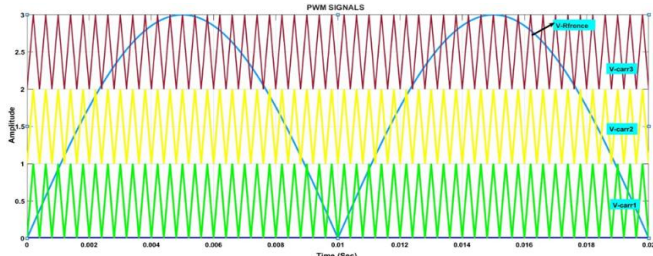


Fig. 12 The rectified wave with the waveforms based on triangle waveforms

### 4. Results and Discussion

This section describes the modeling and verification of the suggested MPPT method. MATLAB/Simulink is used to test the performance of the KC200GT in simulation under various values of irradiance and constant temperature ( $T=25\text{ C}^\circ$ ). The proposed MPPT is compared with conventional P&O, and MP&O methods in terms of oscillation, and tracking speed. The irradiance and temperature profiles used in this simulation are illustrated in Fig. 13. As seen, in this figure, the solar irradiation is varied from low to high

levels for a total simulation time of 3 seconds. An irradiance level with a value of  $500\text{ W/m}^2$  is applied during the time interval (0 - 1sec), and this value is increased from 500 to  $1000\text{ W/m}^2$  from 1 to 2 sec. Finally, this level is decreased again from high to low level to show the response of the MPPTs.

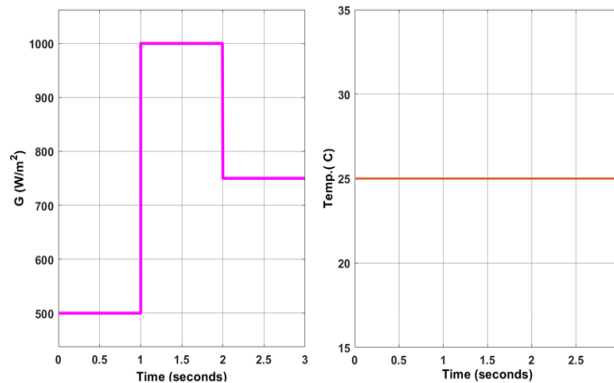


Fig. 13 Irradiance and temperature profiles

Fig. 14 shows the extracted power from the PV module for the proposed GWO-MP&O, MP&O, and P&O MPPT techniques. As seen in this figure, the proposed MPPT offers an excellent response, low oscillation in the output power, and stable dynamic speed. The MP&O is more efficient than the conventional P&O, but it still has issues when the solar irradiance changes quickly. As a result, the tracking efficiency is less than that of the hybrid MPPT, which provides fast speed and a stable power curve at a step change in irradiance.

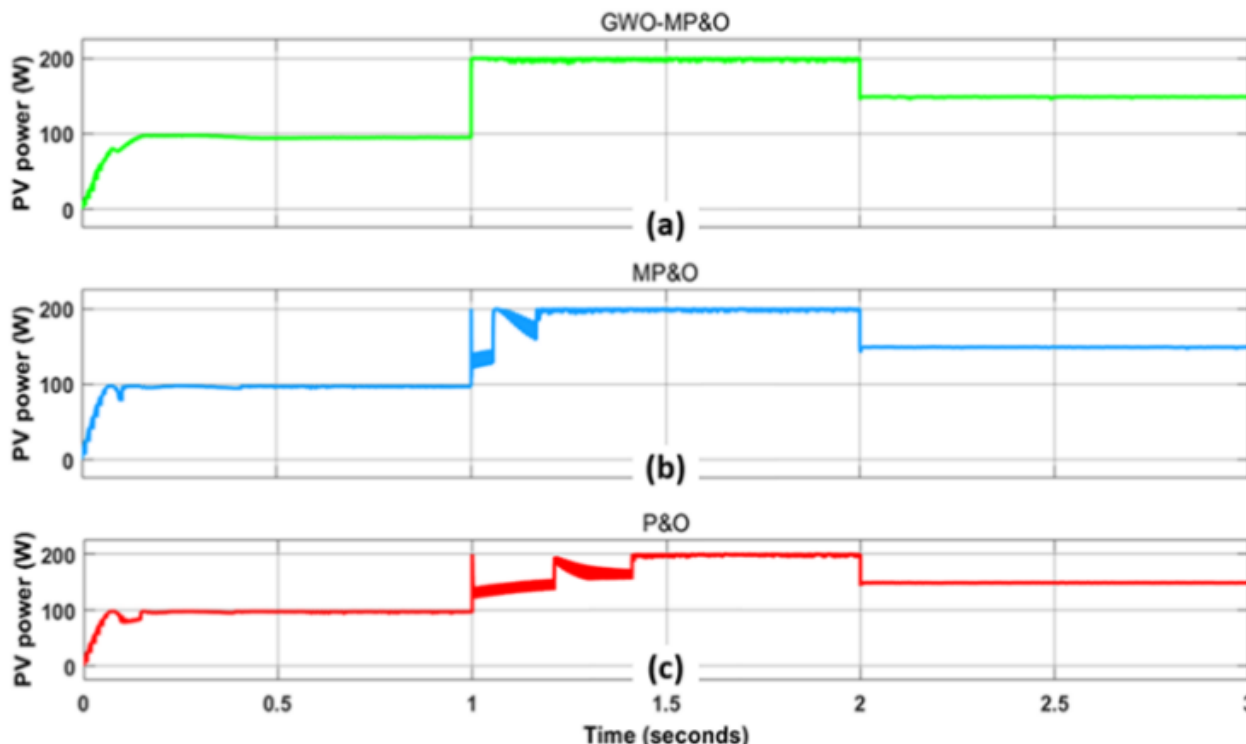


Fig. 14 Power curves of: (a) the proposed GWO-MP&O, (b) MP&O, (c) P&O MPPT methods

The output voltage of the PV module at different weather conditions is seen in Fig. 15. These results were obtained in the three MPPT methods used in this work. As seen, the suggested MPPT methods provide high voltage values and the steady state of this voltage is smooth and it does not influence by changing the solar irradiation against the other MPPT methods.

The conventional P&O has a slow response compared with other methods. Moreover, the output current of the PV module under hybrid MPPT and other methods is displayed in Fig. 16. The suggested MPPT provides a good response, especially at a time interval (1 sec to 2 sec). This variation in the current is small and a high a speed response.

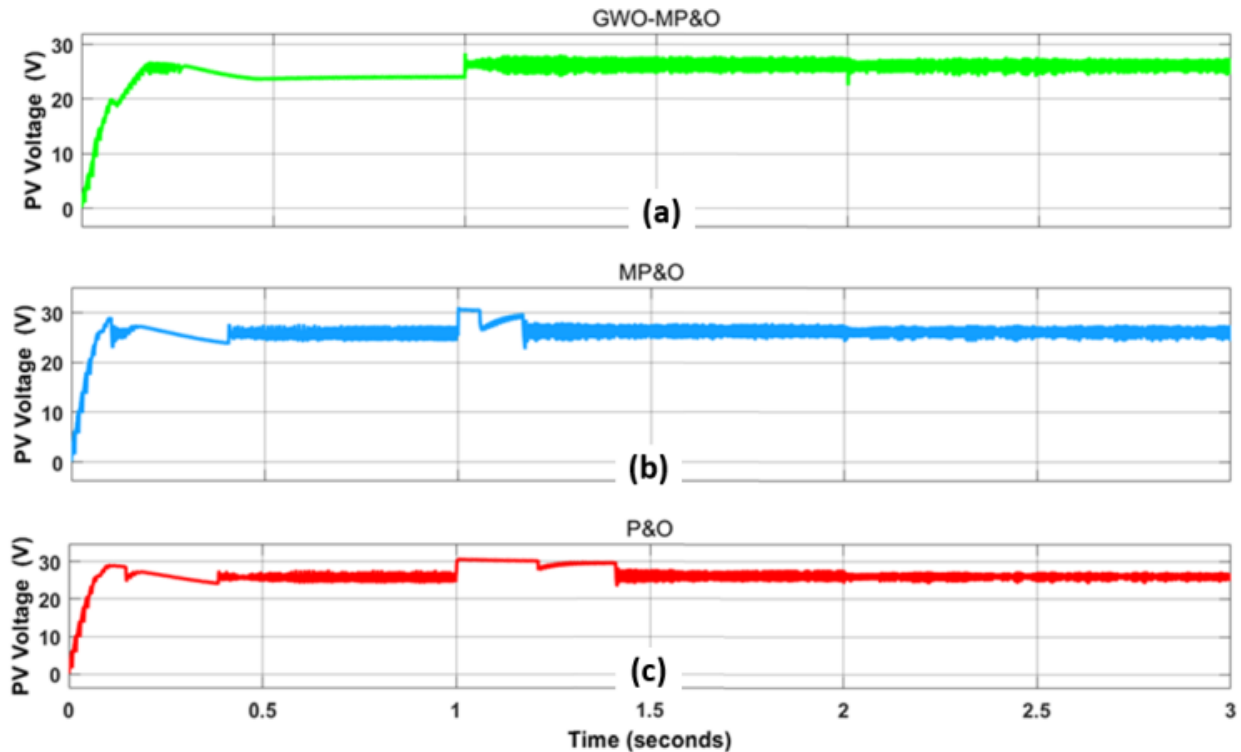


Fig. 15 Output voltage of the PV module from top to bottom: (a) GWO-MP&O, (b) MP&O, (c) P&O methods

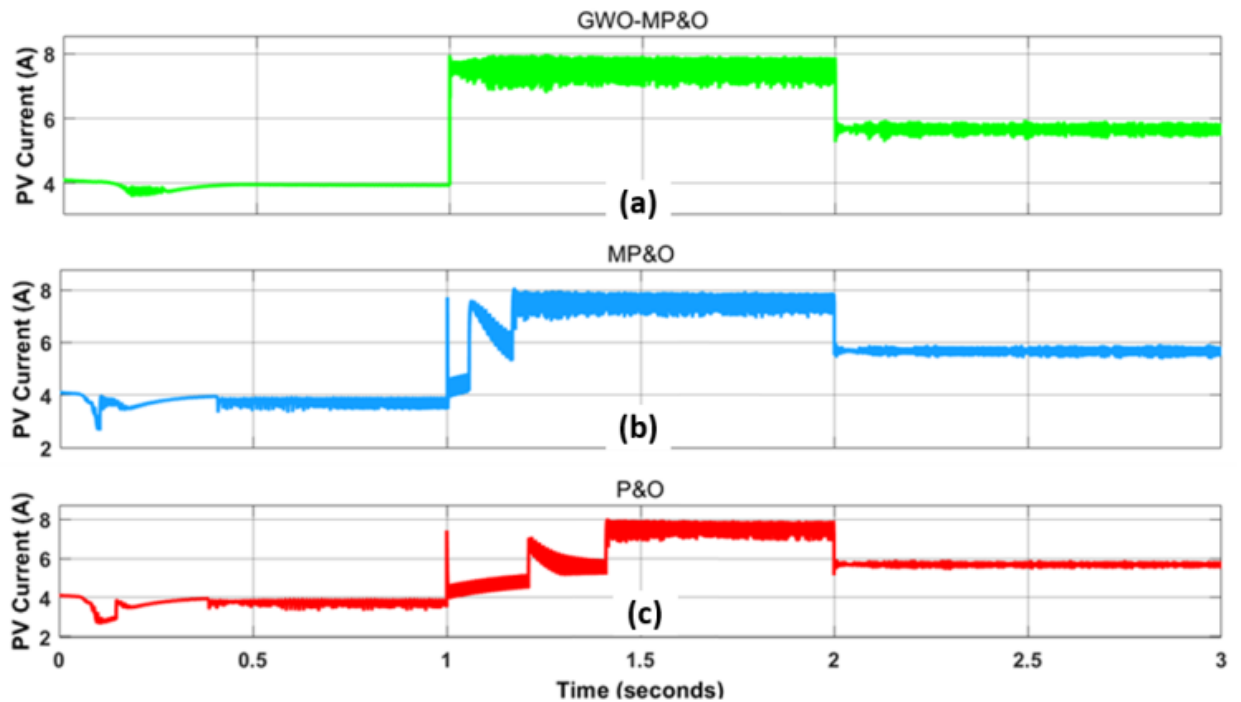


Fig. 16 Output current of the PV module from top to bottom: (a) GWO-MP&O; (b) MP&O; (c) P&O methods

To show the dynamic response of the proposed MPPT, Fig. 17 is used. As seen, the output power from the PV module using the hybrid method is more

smooth and faster than the conventional techniques. This explains the novelty of this work, where the exerted power at different irradiance values is more

stable and has low oscillation around the MPPT. Fig. 17 depicts the panel's power under various irradiance circumstances. As can be seen in the illustration, the extracted power is controlled in accordance with its maximum power at theoretical conditions ( $P_{max} = 200$

W), with a low overshoot and minimum oscillation. On the basis on these findings, it is evident that the suggested MPPT that is presented has superior high smooth power quality, improved stability, and good tracking efficiency.

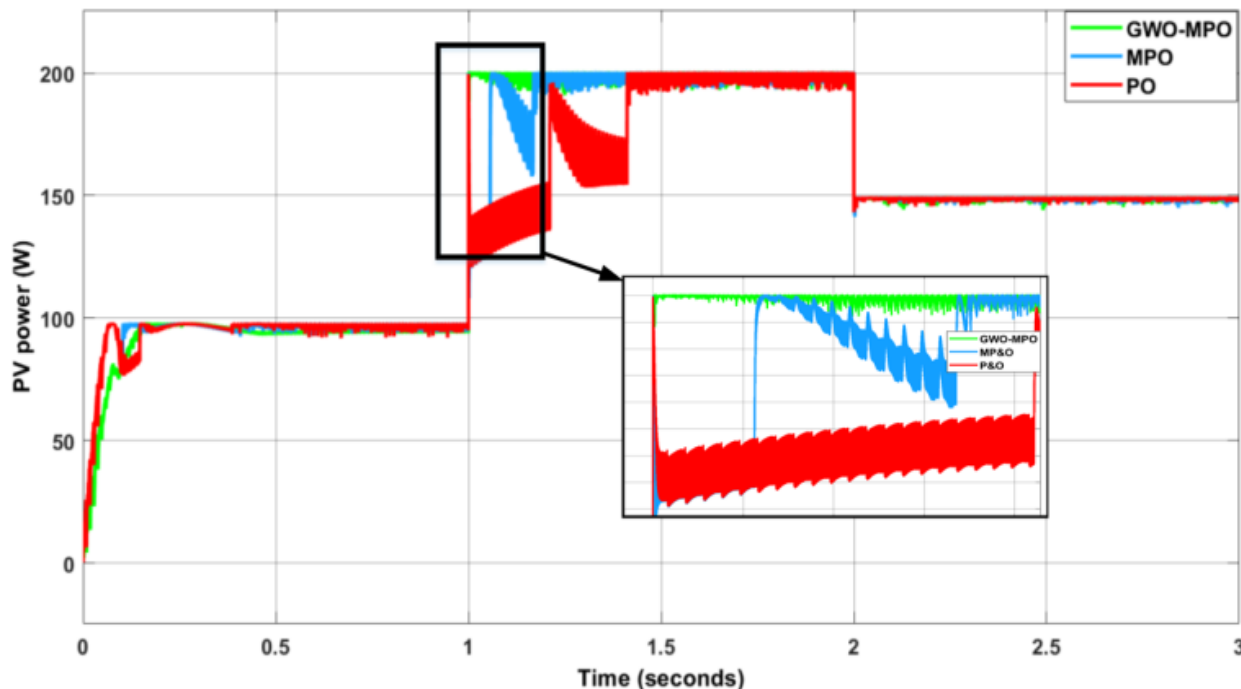


Fig. 17 Comparison between the hybrid MPPT and the other techniques as the same irradiance level

Fig. 18 shows the DC link voltage and the PV voltage at different values, the maximum voltage of the DC bus is obtained under 1000 W/m<sup>2</sup> (100 V). Also, the value of the DC voltage that is used as the input voltage for the proposed MLI is varied according to the solar irradiance or temperature.

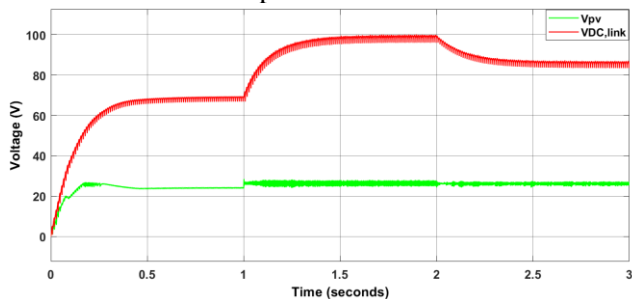


Fig. 18 DC link voltage with PV voltage according to the irradiance profile

The output voltage and current of the proposed MLI used in this work are seen in Fig. 19. As seen, the proposed MLI is tested under a purely resistive load. The seven-level output is achieved according to the value of solar irradiation. The output voltage and current are in the same phase due to the resistive load. The total harmonic distortion (THD) in the output current is obtained based on the Fast Fourier Analysis (FFT) using the MATLAB toolbox. The value of the THD at 1000 W/m<sup>2</sup> is 18.16%, for the RMS current  $i_o = 1.173$  A. The value of the THD at 750 W/m<sup>2</sup> is 18.17%, for the RMS current  $i_o = 1.022$  A. The value

of the THD at 500 W/m<sup>2</sup> is 18.19%, for the RMS current  $i_o = 0.8$  A. To demonstrate the originality of this work, a comparison is made in Table 3 between the performance of the suggested hybrid MPPT and the traditional techniques. The efficiency ( $\eta$ ) is calculated based on the extracted power at each technique according to the maximum power of the datasheet. Additionally, The time response in seconds ( $T_R$ ), average extracted power  $P_{avg}$ , and fluctuation in the power are used to make the comparison. The proposed GWO-MP&O presents excellent efficiency, especially at high irradiances, where an efficiency of 99.7 % is obtained. Although the MP&O presents good efficiency in the higher irradiance it is severe from the high power fluctuation. The time response of the proposed MPPT is very low, and this technique considers faster than both MP&O and P&O at 750 W/m<sup>2</sup> and 1000 W/m<sup>2</sup>.

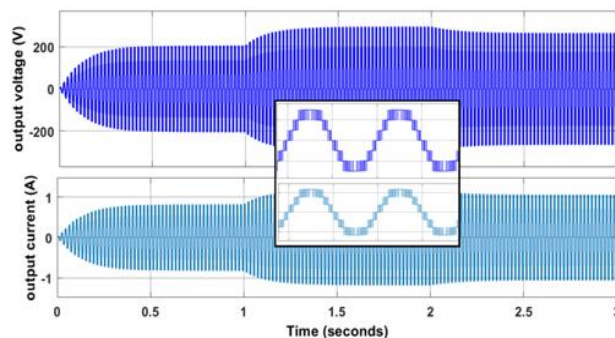


Fig. 19 The output voltage and current of the proposed MLI

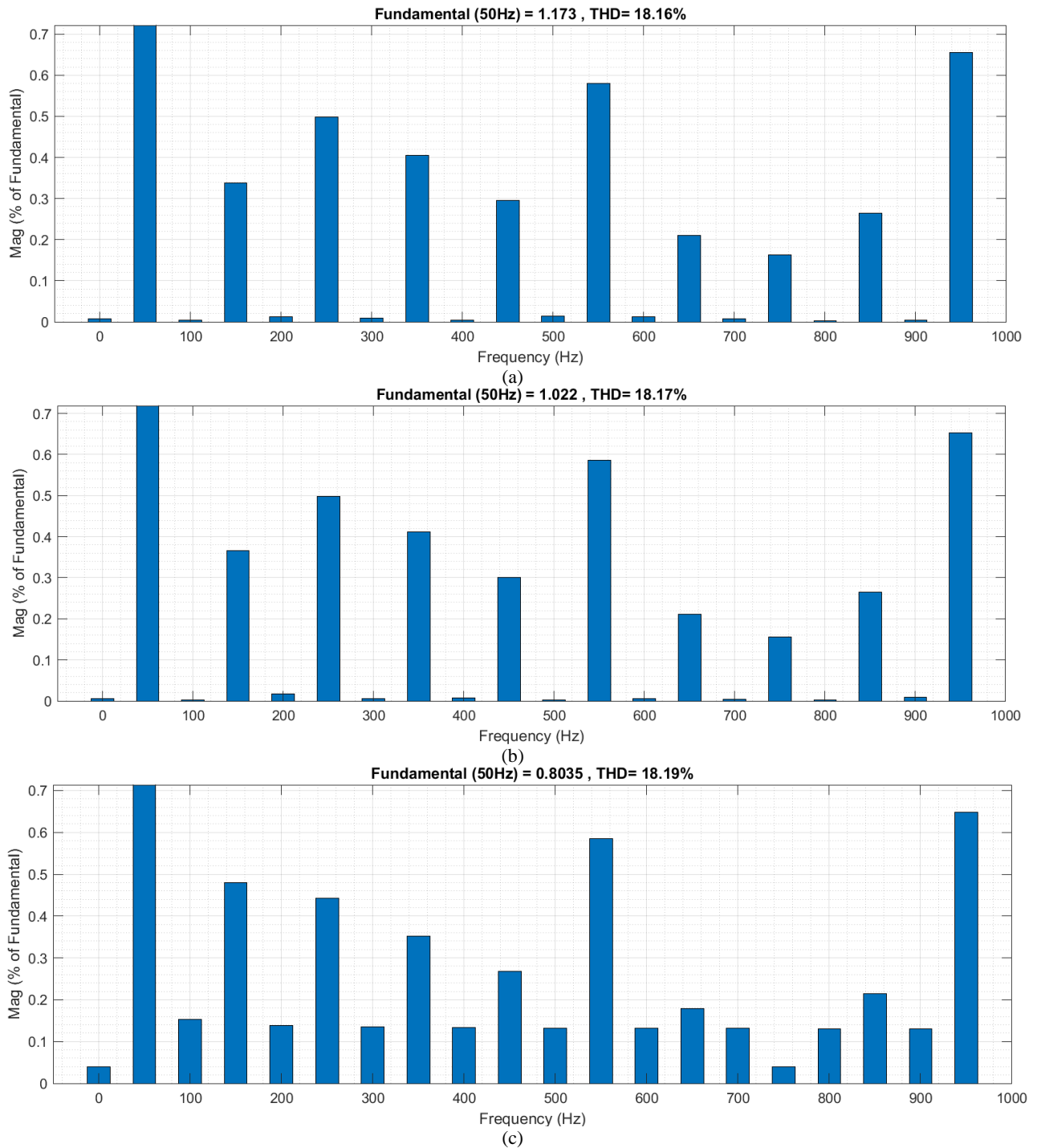


Fig. 20 THD values in the output current at different irradiance (a) THD at 1000 W/m<sup>2</sup> (b) THD at 750 W/m<sup>2</sup> (c) THD at 500 W/m<sup>2</sup>

Table 3 Comparison between the hybrid MPPT and the conventional techniques

G (W/m <sup>2</sup> )	P <sub>max</sub> of panel (W)	MPPT Methods	T <sub>R</sub> (S)	P <sub>avg</sub> (W)	Fluctuation (W)	η(%)
1000	200	P&O	0.45	162.8	6	81.4
		MP&O	0.25	199	4.3	99.5
		Proposed MPPT	0.05	199.7	0.8	99.7
750	150	P&O	0.3	142	5	94.6
		MP&O	0.18	143.2	4	95.4
		Proposed MPPT	0.06	148	1.5	98.6
500	100	P&O	0.17	90.75	6.3	90.7
		MP&O	0.11	96.25	5.34	96.25
		Proposed MPPT	0.13	97.5	2.2	97.5

## 5. Conclusion

This paper aims to propose a new hybrid MPPT method for a PV system to supply a new MLI with a minimum number of switches. The proposed MPPT method is combined from the grey wolf optimizer and the modified P&O MPPT method. The KC200GT PV panel with a rated power of 200 W has been used to show the effectiveness of the suggested method. The MATLAB simulation used to test the performance of the PV system under fast changes in irradiance. The circuit of the MLI is connected to the DC bus via a boost converter. The output power of the PV module is shown using the proposed MPPT, MP&O, and

conventional P&O methods. The obtained results show that the proposed hybrid GWO-MO&O is more efficient and has excellent efficiency of (99.7%) at high irradiance. Compared to the other techniques, the suggested MPPT provides less power oscillation, high speed response, and low power fluctuation. The seven-level output voltage from the proposed MLI with lower THD values in the output current are obtained using this method.

## References

- [1] ABBAS F. A., OBED A. A., QASIM M. A., YAQOUB S.J., and FERAHTIA S. An efficient energy-management strategy for a DC microgrid powered by a photovoltaic/fuel cell/battery/supercapacitor. *Clean Energy*, 2022, 6(6): 827-839. <https://doi.org/10.1093/ce/zkac063>
- [2] YAQOUB S. J., ARNOOS H., QASIM M. A., ALZAHIRANI A., AGYEKUM E., and KAMEL S. (2023). An Optimal Energy Management Strategy for a Photovoltaic/Li-ion Battery Power System for DC Microgrid Application. *Frontiers in Energy Research*, 2010, 10: 1066231. <https://doi.org/10.3389/fenrg.2022.1066231>
- [3] YAQOUB S. J., FERAHTIA S., OBED A. A., REZK H., ALWAN N. T., ZAWBAA H. M., and KAMEL S. Efficient Flatness Based Energy Management Strategy for Hybrid Supercapacitor/Lithium-ion Battery Power System. *IEEE Access*, 2022, 10: 132153-132163. <https://doi.org/10.1109/ACCESS.2022.3230333>
- [4] CECATI C., CIANCETTA F., and SIANO P. A multilevel inverter for photovoltaic systems with fuzzy logic control. *IEEE Transactions on Industrial Electronics*, 2010, 57(12): 4115-4125. <https://doi.org/10.1109/TIE.2010.2044119>
- [5] DAHER S., SCHMID J., and ANTUNES F.L. Multilevel inverter topologies for stand-alone PV systems. *IEEE Transactions on Industrial Electronics*, 2008, 55(7): 2703-2712. <https://doi.org/10.1109/TIE.2008.922601>
- [6] KUMAR S. S., KAVITHA D., AMUDHA A., EMAYAVARAMBAN G., and RAMKUMAR M. S. Analysis of new novelty multilevel inverter configuration with boost converters for a photovoltaic system with MPPT. *Mathematical & Computational Forestry & Natural Resource Sciences*, 2019, 11(1): 1232-1244. [https://www.researchgate.net/publication/326676087\\_Analysis\\_of\\_New\\_Novelty\\_Multilevel\\_Inverter\\_Configuration\\_with\\_Boost\\_Converters\\_for\\_a\\_Photovoltaic\\_System\\_with\\_MPPT](https://www.researchgate.net/publication/326676087_Analysis_of_New_Novelty_Multilevel_Inverter_Configuration_with_Boost_Converters_for_a_Photovoltaic_System_with_MPPT)
- [7] BOUNABI, M., KACED, K., AIT-CHEIKH, M. S., LARBES, C., DAHMANE, Z. E., and RAMZAN, N. Modelling and performance analysis of different multilevel inverter topologies using PSO-MPPT technique for grid connected photovoltaic systems. *Journal of Renewable and Sustainable Energy*, 2018, 10(4): 043507. <https://doi.org/10.1063/1.5043067>
- [8] MINAI A. F., USMANI T., IQBAL A., and MALLICK M. A. Artificial bee colony based solar PV system with Z-source multilevel inverter. Proceedings of the 2020 International Conference on Advances in Computing, Communication & Materials, Dehradun, 2020, pp. 187-193. <https://doi.org/10.1109/ICACCM50413.2020.9213060>
- [9] FEMIA N., PETRONE G., SPAGNUOLO G., and

- VITELLI M. A technique for improving P&O MPPT performances of double-stage grid-connected photovoltaic systems. *IEEE Transactions on Industrial Electronics*, 2009, 56(11): 4473-4482. <https://doi.org/10.1109/TIE.2009.2029589>
- [10] AL-DIAB A., & SOURKOUNIS C. Variable step size P&O MPPT algorithm for PV systems. Proceedings of the 12th International Conference on Optimization of Electrical and Electronic Equipment, Brasov, 2010, pp. 1097-1102. <https://doi.org/10.1109/OPTIM.2010.5510441>
- [11] SALEH A.L., OBED A. A., HASSOUN Z. A., and YAQOUB S.J. Modeling and Simulation of A Low Cost Perturb & Observe and Incremental Conductance MPPT Techniques In Proteus Software Based on Flyback Converter. *IoP Conference Series: Materials Science and Engineering*, 2020, 881(1): 012152. <https://iopscience.iop.org/article/10.1088/1757-899X/881/1/012152/pdf>
- [12] SERA D., MATHE L., KEREKES T., SPATARU S. V., and TEODORESCU, R. On the perturb-and-observe and incremental conductance MPPT methods for PV systems. *IEEE Journal of Photovoltaics*, 2013, 3(3): 1070-1078. <https://doi.org/10.1109/JPHOTOV.2013.2261118>
- [13] BAHARI, M. I., TARASSODI, P., NAEINI, Y. M., KHALILABAD, A. K., and SHIRAZI, P. Modeling and simulation of hill climbing MPPT algorithm for photovoltaic application. Proceedings of the 2016 International Symposium on Power Electronics, Electrical Drives, Automation and Motion, Capri 2016, pp. 1041-1044. <https://doi.org/10.1109/SPEEDAM.2016.7525990>
- [14] DARABAN, S., PETREUS, D., and MOREL, C. A novel MPPT (maximum power point tracking) algorithm based on a modified genetic algorithm specialized on tracking the global maximum power point in photovoltaic systems affected by partial shading. *Energy*, 2014, 74: 374-388. <https://doi.org/10.1016/j.energy.2014.07.001>
- [15] NUGRAHA, D. A., & LIAN, K. L. A novel MPPT method based on cuckoo search algorithm and golden section search algorithm for partially shaded PV system. *Canadian Journal of Electrical and Computer Engineering*, 2019, 42(3): 173-182. <https://doi.org/10.1109/CJECE.2019.2914723>
- [16] AHMED J., & SALAM Z. A soft computing MPPT for PV system based on Cuckoo Search algorithm. Proceedings of the 4th International Conference on Power Engineering, Energy and Electrical Drives, Istanbul, 2013, pp. 558-562. <https://doi.org/10.1109/PowerEng.2013.6635669>
- [17] KOAD R. B., ZOBAA, A. F., and EL-SHAHAT, A. A novel MPPT algorithm based on particle swarm optimization for photovoltaic systems. *IEEE Transactions on Sustainable Energy*, 2016, 8(2): 468-476. <https://doi.org/10.1109/TSTE.2016.2606421>
- [18] LIAN, K.L., JHANG, J. H., and TIAN, I. S. A maximum power point tracking method based on perturb-and-observe combined with particle swarm optimization. *IEEE Journal of Photovoltaics*, 2014, 4(2): 626-633. <https://doi.org/10.1109/JPHOTOV.2013.2297513>
- [19] TITRI S., LARBES C., TOUMI K. Y., and BENATCHBA K. A new MPPT controller based on the Ant colony optimization algorithm for Photovoltaic systems under partial shading conditions. *Applied Soft Computing*, 2017, 58: 465-479. <https://doi.org/10.1016/j.asoc.2017.05.017>

- [20] REZK H., FATHY A., and ABDELAZIZ A. Y. A comparison of different global MPPT techniques based on meta-heuristic algorithms for photovoltaic system subjected to partial shading conditions. *Renewable and Sustainable Energy Reviews*, 2017, 74: 377-386. <https://doi.org/10.1016/j.rser.2017.02.051>
- [21] GONZÁLEZ-CASTAÑO, C., RESTREPO, C., KOURO, S., and RODRIGUEZ, J. MPPT algorithm based on artificial bee colony for PV system. *IEEE Access*, 2021, 9: 43121-43133. <https://doi.org/10.1109/ACCESS.2021.3066281>
- [22] PILAKKAT D., & KANTHALAKSHMI S. Single phase PV system operating under Partially Shaded Conditions with ABC-PO as MPPT algorithm for grid connected applications. *Energy Reports*, 2020, 6: 1910-1921. <https://doi.org/10.1016/j.egy.2020.07.019>
- [23] SUNDARESWARAN K., KUMAR V. V., and PALANI S. Application of a combined particle swarm optimization and perturb and observe method for MPPT in PV systems under partial shading conditions. *Renewable Energy*, 2015, 75: 308-317. <https://doi.org/10.1016/j.renene.2014.09.044>
- [24] MIRJALILI S., MIRJALILI S. M., and LEWIS A. Grey wolf optimizer. *Advances in Engineering Software*, 2014, 69: 46-61. <https://doi.org/10.1016/j.advengsoft.2013.12.007>
- [25] MOHANTY S., SUBUDHI B., and RAY P. K. A grey wolf-assisted perturb & observe MPPT algorithm for a PV system. *IEEE Transactions on Energy Conversion*, 2016, 32(1): 340-347. <https://doi.org/10.1109/TEC.2016.2633722>
- [26] YAQOUB S. J., SALEH A. L., MOTAHHIR S., AGYEKUM E. B., NAYYAR A., and QURESHI B. Comparative study with practical validation of photovoltaic monocrystalline module for single and double diode models. *Scientific Reports*, 2021, 11(1): 1-14. <https://doi.org/10.1038/s41598-021-98593-6>
- [27] YAQOUB S. J., MOTAHHIR S., and AGYEKUM E. B. A new model for a photovoltaic panel using Proteus software tool under arbitrary environmental conditions. *Journal of Cleaner Production*, 2022, 333: 130074. <https://doi.org/10.1016/j.jclepro.2021.130074>
- [28] MOTAHHIR S., EL GHZIZAL A., SEBTI S., and DEROUICH A. Modeling of photovoltaic system with modified incremental conductance algorithm for fast changes of irradiance. *International Journal of Photoenergy*, 2018, 2018: 3286479. <https://doi.org/10.1155/2018/3286479>
- [29] MAO M., CUI L., ZHANG Q., GUO K., ZHOU L., and HUANG H. Classification and summarization of solar photovoltaic MPPT techniques: A review based on traditional and intelligent control strategies. *Energy Reports*, 2020, 6: 1312-1327. <https://doi.org/10.1016/j.egy.2020.05.013>
- [30] BENZAOUIA M., HAJJI B., RABHI A., MELLIT A., BENSLIMANE A., and DUBOIS A. M. Energy management strategy for an optimum control of a standalone photovoltaic-batteries water pumping system for agriculture applications. *Proceedings of the International Conference on Electronic Engineering and Renewable Energy*, Saida, 2020, pp. 855-868.
- S.J., 和 FERAHTIA S. 由光伏/燃料电池/电池/超级电容器供电的直流微电网的高效能源管理策略. *清洁能源*, 2022年, 6(6): 第 827-839 页. <https://doi.org/10.1093/ce/zkac063>
- [2] YAQOUB S. J., ARNOOS H., QASIM M. A., ALZHRANI A., AGYEKUM E., 和 KAMEL S. (2023). 用于直流微电网应用的光伏/锂离子电池电源系统的最佳能量管理策略. *能源研究前沿*, 2010, 10: 文章1066231. <https://doi.org/10.3389/fenrg.2022.1066231>
- [3] YAQOUB S. J., FERAHTIA S., OBED A. A., REZK H., ALWAN N. T., ZAWBAA H. M., 和 KAMEL S. 混合超级电容器/锂离子电池电源系统的基于高效平坦度的能量管理策略. *电气和电子工程师协会使用权*, 2022年, 10: 第 132153-132163 页. <https://doi.org/10.1109/ACCESS.2022.3230333>
- [4] CECATI C., CIANCETTA F., 和 SIANO P. 具有模糊逻辑控制的光伏系统多级逆变器. *电气和电子工程师学会工业电子交易*, 2010年, 57(12): 第 4115-4125 页. <https://doi.org/10.1109/TIE.2010.2044119>
- [5] DAHER S., SCHMID J., 和 ANTUNES F.L. 用于独立光伏系统的多级逆变器拓扑. *电气和电子工程师学会工业电子交易*, 2008年, 55(7): 第 2703-2712 页. <https://doi.org/10.1109/TIE.2008.922601>
- [6] KUMAR S. S., KAVITHA D., AMUDHA A., EMAYAVARAMBAN G., 和 RAMKUMAR M. S. 具有最大功率点跟踪功能的光伏系统升压转换器的新型多级逆变器配置分析. *数学与计算林业与自然资源科学*, 2019年, 11(1): 第 1232-1244 页. [https://www.researchgate.net/publication/326676087\\_Analysis\\_of\\_New\\_Novelty\\_Multilevel\\_Inverter\\_Configuration\\_with\\_Boost\\_Converters\\_for\\_a\\_Photovoltaic\\_System\\_with\\_MPPT](https://www.researchgate.net/publication/326676087_Analysis_of_New_Novelty_Multilevel_Inverter_Configuration_with_Boost_Converters_for_a_Photovoltaic_System_with_MPPT)
- [7] BOUNABI, M., KACED, K., AIT-CHEIKH, M. S., LARBES, C., DAHMANE, Z. E., 和 RAMZAN, N. 使用粒子群优化对不同的多级逆变器拓扑进行建模和性能分析- 并网光伏系统的最大功率点跟踪技术. *可再生和可持续能源杂志*, 2018, 10(4): 文章043507. <https://doi.org/10.1063/1.5043067>
- [8] MINAI A. F., USMANI T., IQBAL A., 和 MALLICK M. A. 具有Z源多电平逆变器的基于人工蜂群的太阳能光伏系统. *2020年计算、通信和材料进展国际会议论文集*, 台拉登, 2020年, 第 187-193 页. <https://doi.org/10.1109/ICACCM50413.2020.9213060>
- [9] FEMIA N., PETRONE G., SPAGNUOLO G., 和 VITELLI M.

#### 参考文献:

[1] ABBAS F. A., OBED A. A., QASIM M. A., YAQOUB

- 一种提高双级并网光伏系统扰动观察最大功率点跟踪性能的技术。电气和电子工程师学会工业电子汇刊, 2009年, 56(11): 第 4473-4482 页。  
<https://doi.org/10.1109/TIE.2009.2029589>
- [10] AL-DIAB A., 和 SOURKOUNIS C. 可变步长扰动和观察光伏系统的最大功率点跟踪算法。第12届电气和电子设备优化国际会议论文集, 布拉索夫, 2010年, 第 1097-1102 页。  
<https://doi.org/10.1109/OPTIM.2010.5510441>
- [11] SALEH A.L., OBED A. A., HASSOUN Z. A., 和 YAQOOB S.J. 基于反激式转换器的变形杆菌软件中低成本扰动观察和增量电导最大功率点跟踪技术的建模和仿真。物理研究所系列会议: 材料科学与工程, 2020, 881(1): 文章 012152. <https://iopscience.iop.org/article/10.1088/1757-899X/881/1/012152/pdf>
- [12] SERA D., MATHE L., KERESKES T., SPATARU S. V., 和 TEODORESCU, R. 关于光伏系统的扰动观察和增量电导最大功率点跟踪方法。电气电子工程师学会 光伏学报, 2013, 3(3): 第1070-1078页. <https://doi.org/10.1109/JPHOTOV.2013.2261118>
- [13] BAHARI, M. I., TARASSODI, P., NAEINI, Y. M., KHALILABAD, A. K., 和 SHIRAZI, P. 光伏应用爬山最大功率点跟踪算法建模与仿真2016年电力电子、电气驱动、自动化和运动国际研讨会论文集, 卡普里2016, 第 1041-1044 页。  
<https://doi.org/10.1109/SPEEDAM.2016.7525990>
- [14] DARABAN, S., PETREUS, D., 和 MOREL, C. 一种基于改进遗传算法的新型最大功率点跟踪算法, 专门用于跟踪受部分遮挡影响的光伏系统中的全局最大功率点。能源, 2014年, 74: 第 374-388 页。  
<https://doi.org/10.1016/j.energy.2014.07.001>
- [15] NUGRAHA, D. A., 和 LIAN, K. L. 一种基于布谷鸟搜索算法和黄金分割搜索算法的局部遮挡光伏系统最大功率点跟踪新方法。加拿大电气与计算机工程杂志, 2019年, 42(3): 第 173-182 页。  
<https://doi.org/10.1109/CJECE.2019.2914723>
- [16] AHMED J., 和 SALAM Z. 基于布谷鸟搜索算法的光伏系统软计算最大功率点跟踪。第四届电力工程、能源和电气驱动国际会议论文集, 伊斯坦布尔, 2013年, 第 558-562 页。  
<https://doi.org/10.1109/PowerEng.2013.6635669>
- [17] KOAD R. B., ZOBAA, A. F., 和 EL-SHAHAT, A. 一种新的基于粒子群优化的光伏系统最大功率点跟踪算法。电气和电子工程师学会可持续能源汇刊, 2016年, 8(2): 第 468-476 页。  
<https://doi.org/10.1109/TSTE.2016.2606421>
- [18] LIAN, K.L., JHANG, J. H., 和 TIAN, I. S. 一种基于扰动观察结合粒子群优化的最大功率点跟踪方法。电气电子工程师学会光伏学报, 2014, 4(2): 第626-633页. <https://doi.org/10.1109/JPHOTOV.2013.2297513>
- [19] TITRI S., LARBES C., TOUMI K. Y., 和 BENATCHBA K. 一种基于蚁群优化算法的新型最大功率点跟踪控制器, 适用于部分遮挡条件下的光伏系统。应用软计算, 2017年, 58: 第 465-479 页。  
<https://doi.org/10.1016/j.asoc.2017.05.017>
- [20] REZK H., FATHY A., 和 ABDELAZIZ A. Y. 基于元启发式算法的不同全球电气和电子工程师协会技术的比较, 用于受部分遮挡条件影响的光伏系统。可再生和可持续能源评论, 2017年, 74: 第 377-386 页。  
<https://doi.org/10.1016/j.rser.2017.02.051>
- [21] GONZÁLEZ-CASTAÑO, C., RESTREPO, C., KOURO, S., 和 RODRIGUEZ, J. 基于人工蜂群的光伏系统最大功率点跟踪算法电气和电子工程师协会使用权, 2021年, 9: 第 43121-43133 页。  
<https://doi.org/10.1109/ACCESS.2021.3066281>
- [22] PILAKKAT D., & KANTHALAKSHMI S. 单相光伏系统在部分遮荫条件下运行, 人工蜂群集成扰动和观察作为电网连接应用的最大功率点跟踪算法。能源报告, 2020年, 6: 1910-1921.  
<https://doi.org/10.1016/j.egy.2020.07.019>
- [23] SUNDARESWARAN K., KUMAR V. V., 和 PALANI S. 结合粒子群优化和扰动观察方法在部分遮挡条件下光伏系统最大功率点跟踪中的应用。可再生能源, 2015年, 75: 第 308-317 页。  
<https://doi.org/10.1016/j.renene.2014.09.044>
- [24] MIRJALILI S., MIRJALILI S. M., 和 LEWIS A. 灰狼优化器。工程软件进展, 2014年, 69: 第 46-61 页。  
<https://doi.org/10.1016/j.advengsoft.2013.12.007>
- [25] MOHANTY S., SUBUDHI B., 和 RAY P. K. 灰狼辅助扰动观察光伏系统最大功率点跟踪算法。电气和电子工程师协会能源转换汇刊, 2016年, 32(1): 第 340-347 页. <https://doi.org/10.1109/TEC.2016.2633722>
- [26] YAQOOB S. J., SALEH A. L., MOTAHHIR S., AGYEKUM E. B., NAYYAR A., 和 QURESHI B. 单二极管和双二极管模型光伏单晶模块实际验证的比较研究。科学报告, 2021年, 11(1): 第 1-14 页。  
<https://doi.org/10.1038/s41598-021-98593-6>
- [27] YAQOOB S. J., MOTAHHIR S., 和 AGYEKUM E. B.

在任意环境条件下使用变形杆菌软件工具的光伏面板新模型。清洁生产杂志，2022年，333：文章130074。

<https://doi.org/10.1016/j.jclepro.2021.130074>

[28] MOTAHHIR S., EL GHZIZAL A., SEBTI S., 和 DEROUICH A.

使用改进的增量电导算法对光伏系统进行建模以实现辐照度的快速变化。国际光能杂志，2018，2018：文章3286479。 <https://doi.org/10.1155/2018/3286479>

[29] MAO M., CUI L., ZHANG Q., GUO K., ZHOU L., 和 HUANG H.

太阳能光伏MPPT技术的分类和总结：基于传统和智能控制策略的综述。能源报告，2020年，第 6 期：第 1312-1327 页。 <https://doi.org/10.1016/j.egy.2020.05.013>

[30] BENZAOUIA M., HAJJI B., RABHI A., MELLIT A., BENSLIMANE A., 和 DUBOIS A. M.

用于农业应用的独立光伏电池水泵系统最佳控制的能源管理策略。电子工程与可再生能源国际会议论文集，斋田，2020年，第 855-868 页。